IEEE Access
Multidisciplinary | Rapid Review | Open Access Journal

Received 4 April 2023, accepted 20 April 2023, date of publication 26 April 2023, date of current version 4 May 2023.

Digital Object Identifier 10.1109/ACCESS.2023.3270803

RESEARCH ARTICLE

State-Based Decoding of Continuous Hand Movements Using EEG Signals

SEYYED MOOSA HOSSEINI AND VAHID SHALCHYAN

Neuroscience & Neuroengineering Research Laboratory, Biomedical Engineering Department, School of Electrical Engineering, Iran University of Science & Technology, Tehran, 16846-13114, Iran

Corresponding author: Vahid Shalchyan (shalchyan@iust.ac.ir)

This work involved human subjects or animals in its research. Approval of all ethical and experimental procedures and protocols was granted by the Ethics Committee of the Iran University of Medical Sciences under Approval No. IR.IUMS.REC.1400.382.

ABSTRACT Recently, the advent of the non-invasive brain-computer interface (BCI) for continuous decoding of upper limb motions opens a new horizon for motor-disabled people. However, the performance of discrete-decoding BCIs based on discriminating different brain states are still more robust. In this study, we aimed to cascade a discrete state decoder with a continuous decoder to enhance the prediction of hand trajectories. EEG data were recorded from nine healthy subjects performing a center-out task with four orthogonal targets on the horizontal plane. The pre-movement data of each trial has been used for training a binary discrete decoder which identifies the axis of the movement based on common spatial pattern (CSP) features. Two non-parametric continuous decoders based on Gaussian process regression (GPR) have been designed for continuous decoding of hand movements along each axis using the envelope features of EEG signals in six frequency bands. In addition to those four principal orthogonal targets, some targets at random directions on the horizontal plane were recorded to evaluate the generalizability of the proposed model. The discrete decoder attained the average binary classification of 97.1% for discriminating movement along the x-axis and y-axis. The proposed state-based method achieved the mean correlation coefficient of 0.54 between actual and predicted trajectories for principal targets over all subjects. The trajectories of random targets were also decoded with a mean correlation of 0.37. The generalizability of the proposed paradigm proved by the findings of this study could open new possibilities in developing novel types of neuroprostheses for rehabilitation purposes.

INDEX TERMS Brain–computer interface, continuous decoding, electroencephalography, Gaussian process regression, state-based decoding.

I. INTRODUCTION

The main objective of brain-computer interfaces (BCIs) is to translate brain activity patterns into meaningful control commands which enables motor-deficient people to interact with the environment via an external device such as a computer or a prosthetic limb [1], [2]. The application of the BCI system is not only confined to helping paralyzed patients, it also includes mental-state monitoring, stroke rehabilitation, gaming, and entertainment [3], [4], [5], [6]. However, restoring upper limb movement via circumventing the dysfunctional neuromuscular pathway is of utmost importance in the neuroengineering and rehabilitation fields. Hence, Inferring hand movement kinematics from brain recordings has been investigated in many studies. Georgopoulos and his colleagues proved that the direction of hand movement can be predicted from the activity of population motor neurons in the arm area of the primate motor cortex [7]. Taylor et al. proposed an online closed-loop BCI based on decoding continuous trajectory from spiking activities which enabled the monkey subjects to control the position of a cursor in real time [8]. Several studies are reporting successful trajectory decoding BCIs based on spiking activities of human subjects with sever-motor disabilities [9], [10], [11]. Other types of

The associate editor coordinating the review of this manuscript and approving it for publication was Humaira Nisar.

invasively-recorded brain activities such as local field potentials (LFP) or electrocorticography (ECoG) have already been used as an information source for decoding upper limb kinematics [12], [13]. The crucial advantage of invasive BCIs is their acceptable performance. However, it comes at the expense of requiring surgery which involves the risk of brain tissue scarring and post-surgical infections. Additionally, the long-term signal stability of chronically-implanted electrodes is a matter of discussion [14], [15]. These drawbacks limit the applications of invasive BCIs. Therefore, there is ongoing interest in the development of trajectory decoding BCIs based on non-invasive modalities such as EEG recordings.

The feasibility of using non-invasive brain recordings for continuous decoding of hand movement parameters was first proved in a paper by Bradbery et al. [16] where the velocity trajectories of hand movements were reconstructed from low-delta EEG potentials in a 3D center-out task. The problem of estimating hand motion parameters from EEG signals has attracted widespread attention recently [17], [18], [19], [20], [21]. Korik et al. [18] demonstrated the role of band-power features from mu, beta, and low-gamma frequency bands in EEG-based motion trajectory prediction. They obtained a maximum of 0.4 Pearson correlation coefficient between the actual and reconstructed trajectories. Mondini et al [19] exploited the low-delta EEG potentials to reconstruct hand motion trajectories in a pursuit-tracking task. They achieved the mean correlation coefficient of 0.32 between prediction and actual movement trajectories at their best scenario. In an exhaustive study, Ubeda et al. [17] examined the problem of movement decoding based on EEG recordings from the discrete and continuous perspective in a center-out-reaching task with eight targets. Their findings showed that movement trajectories could be reconstructed via a linear regression model with statistical significance from low-frequency contents of EEG signals. Nevertheless, they concluded that the classification of movement direction may be a more reliable and appropriate approach compared to continuous decoding of hand position due to the poor performance of regression model prediction.

Discrete decoding of hand movements from EEG data during the movement execution period has been studied comprehensively in the literature [17], [22], [23], [24]. In a study by Waldert [22], the four directions of a center-out paradigm were decoded with an accuracy of 55% using EEG power spectrum features. Robinson et al [23] exploited a regularized wavelet common spatial pattern to extract features from EEG signals and achieved a four-class classification accuracy of 80.24% for discriminating hand directions in a center-out experiment. The movement discriminative capability of EEG data from pre-movement interval was also confirmed [25], [26], [27]. Lew et al. [26] verified the feasibility of using EEG data before the onset of movement for hand directions classification with an accuracy of 76% in a four-class scenario. The preparation phase of a center-out task was also analyzed in [27] for binary classification of left versus right and up versus down movements with the highest attained discrimination accuracy of 85%. Compared to continuous decoding, the overall results of discrete decoding studies based on EEG recordings are more competent for real-life applications.

In the present work, a novel methodology based on the combination of a discrete decoder and a nonparametric nonlinear continuous decoder has been proposed to enhance the overall performance of hand movement trajectory prediction from EEG recordings. For this sake, EEG data were recorded from nine healthy subjects performing a center-out-reaching task with four orthogonal targets on the horizontal plane. In addition to the principal targets located on two orthogonal axes, several trials with targets placed in random directions (i.e. outside the orthogonal axes) on the horizontal plane have been recorded from each subject. The random targets required simultaneous movement along both orthogonal axes. The objective behind recording random targets was to assess the generalizability of the proposed model trained only on the four orthogonal targets. The proposed approach is called state-based because it first determines the axis in which the movement happened (i.e. discrete state) and then exploits the corresponding proper regressor. The discrete state detection is based on power features extracted from slow cortical potentials (SCPs) which have been known to be informative for direction decoding even before the onset of movement [26], [27]. A common spatial pattern (CSP) feature extraction method alongside a support vector machine (SVM) classifier with a nonlinear kernel has been exploited for designing the discrete state decoder. Gaussian process regression (GPR) was employed for continuous decoding of hand positions using the envelope features of EEG signals extracted from six frequency sub-bands. Our findings revealed that the proposed method offers statistically significant results on both principal and random targets compared to the conventional method which is not state-based. The state-based approach has been employed in some movement parameter estimation studies based on invasive brain recordings [28], [29]. However, as far as we know, this is the first study that investigates the performance of a state-based decoder in a generalized EEG center-out task with random targets aiming to improve the hand trajectory predictions.

The rest of the paper is prepared as follows: Materials and Methods are presented in Section II. It comprehensively describes data acquisition, experimental task, and methodology including discrete and continuous decoder design. Section III is dedicated to the results. Discussions are summarized in Section IV. Finally, Section V is left for conclusions.

II. MATERIALS AND METHODS

A. PARTICIPANTS AND EQUIPMENT

Nine healthy right-handed male subjects between the ages of 25-36 with correct or corrected-to-normal vision participated in this study. All subjects had no history of epilepsy, neurological diseases, mental disorders, or head injury.

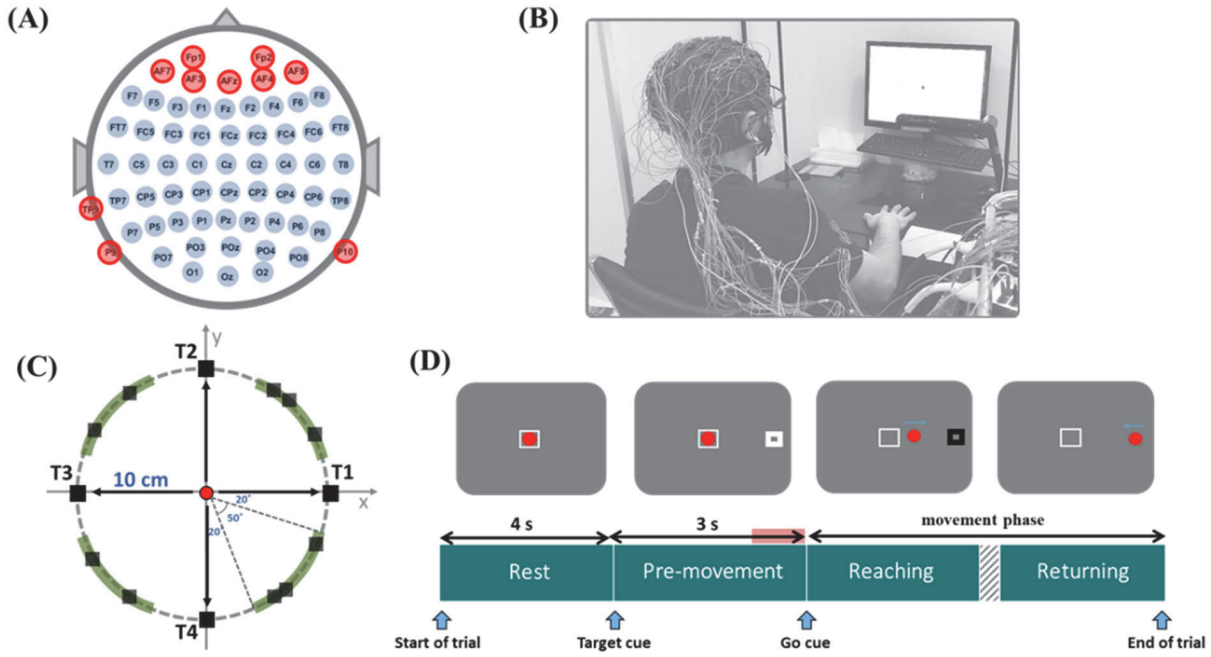

FIGURE 1. (A) EEG electrode montage showing recording channels. The channels denoted in red were discarded from the analysis. (B) A participant performing the task in the experimental environment. (C) Targets layout. The principal targets are denoted with T1, T2, T3, and T4. The random targets were placed randomly over four quadrants in the area designated by green color. (D) Timeline for the experimental task alongside the cue screen pictures of the experiment. The thick red line shows the 500 ms interval used for state detection.

The overall health of subjects were check by a general physician before recording session. The experiment was carried out in one session for each subject. All the procedures were approved by the Ethics Committee of the Iran University of Medical Sciences (Ethics ID: IR.IUMS.REC.1400.382.). All subjects were informed about the details of the experimental task and gave written consent in accordance with the Declaration of Helsinki prior to the data acquisition session. Data acquisition took place at the National Brain mapping Lab (NBML) at the University of Tehran, Iran.

The sufficient number of subjects for our experiment was determined based on statistical power analysis which was performed using G*power software [30]. Statistical power analysis describes the relationship of four factors of statistical hypothesis testing: sample size (N), significance criterion (α), effect size (d), and statistical power. Statistical power is the probability that a statistical hypothesis test correctly rejects the null hypothesis. We performed a power analysis to verify whether the number of participants in our study was sufficient to show the superiority of the state-based approach over the conventional method. Considering the results of the proposed method and conventional method, the effect size calculated by G*power was equal to d=2.13. Effect size measure represents the magnitude of a relationship between variables. Given the calculated effect size, $\alpha = 0.05$, and Power $= 0.9$, the minimum number of subjects calculated by G*Power software for the Wilcoxon signed-rank test is equal to seven. Thus, in our experiment with nine subjects, our sample size was enough to justify the results of the statistical test.

A g.HIamp device (g.Tec, GmbH, Austria) equipped with 63 active electrodes was used for EEG data recording at a sampling rate of 512 Hz. The electrode placement was according to the extended international 10-20 system with the ground electrode positioned at Fpz and the reference electrode placed at the right mastoid. The EEG electrode montage is illustrated in Fig. 1(A). The electrooculogram (EOG) signals were captured simultaneously with three additional passive patch electrodes positioned at the right eye's superior, inferior, and outer canthi. The position of the right hand's palm was recorded via a LeapMotion controller (LeapMotion Inc. USA). The hand movement was sampled at 115Hz. To reduce the sensor noise, the LeapMotion signals were smoothed with a low-pass Butterworth filter (zero-phase, fourth order, and cutoff frequency at 1Hz). Fig. 1(B) portrays a subject performing the task in the experimental environment.

B. EXPERIMENTAL TASK

To address the main objective of the study, a cue-based center-out reaching task was designed. The task required hand-reaching movement towards four principal targets positioned on two orthogonal axes at an equal distance of 10cm from a center position called home located on the horizontal plane. This design is in line with the conventional center-out task which is well-known in the literature [23], [25], [31]. To evaluate the generalizability of the proposed method, we incorporated different random targets happening in random directions into our center-out task. The random targets

would happen at directions that are at least 20 degrees away from principal orthogonal axes. In other words, the directions of random targets were drawn from a uniform distribution which its values happen at [20° 70°], [110° 160°], [200° 250°], and [290 340°] intervals. The random targets were distributed uniformly over all four quadrants of the horizontal coordinate plane with the home position considered as the origin. Hence, there are two types of targets in this study, principal targets for training the model and random targets for assessing the model's generalizability. Fig. 1(C) represents the task targets' positions layout which shows the orthogonal principal targets and the area in which the random targets happen. Four principal targets are labeled T1, T2, T3, and T4. All targets whether principal or random require 10 cm hand displacement from the origin to be reached.

The timeline for the experimental task is depicted in Fig.1(D). The experiment was conducted as follows: the participants were seated comfortably on a chair positioned 50cm away from the computer screen with their arms resting on the table. To reduce the friction with the table surface during task execution, the subjects were asked to place their right hand on a mouse pad. At the beginning of each trial, the right-hand palm position of the subjects was mapped into a red circle cursor at the home position on the computer screen. The home position was denoted with a thin white rectangle at the center of the screen. The hand position data were recorded via LeapMotion device which was placed on a leg 25 cm above the table surface. Every trial began with a 4 seconds rest period. Then, a target denoted by a bold white rectangle appeared at one of the four principal target positions or a random target position. After 3 seconds, the white rectangle turned black indicating the go cue. The subjects were instructed to start reaching the target after the go cue. When the target was touched by the cursor, its color changed to white and disappeared after 400ms (return cue). Then, the subjects returned the cursor to the central position to end the trial. So the hand movement in each trial consists of reaching and returning phases. If the subject could not complete the movement within 10 seconds after the go cue, the trial was terminated and discarded. The graphical user interface (GUI) of the task was implemented via PsychToolbox 3 in MATLAB 2019b (The MathWorks, Inc.).

The experiment was completed in one session for each subject. Each session consists of four data recording blocks. In each block, the subjects performed 40 trials toward principal targets (ten attempts for each principal target) and six trials toward random targets. The order of presenting trials to the subjects was random in each recording block. A break interval of 2-3 minutes was applied between recoding blocks. In total, each subject performed 160 principal target trials and 24 random target trials. The number of random target trials was 15% of the total number of principal target trials. The random target trials were only used for testing the generalization capability of the algorithm. They were not intended for training the models.

In this study, the 500 ms of data before the go cue was used for state-decoder design. Although the subjects were not allowed to move their hand in the pre-movement interval, the brain activity in this interval carried discriminative information for direction decoding [25], [27]. The data in the movement phase including reaching and returning were employed for designing a continuous decoder as well (Fig. 1(D)).

C. PREPROCESSING DATA

The raw EEG data were band-pass filtered using a zero-phase fourth-order Butterworth filter with 0.2-45Hz bandwidth. The EOG signals were also bandpass filtered in the 0.5-5Hz frequency range [32]. The powerline interference was eliminated with a notch filter at 50 Hz. Next, independent component analysis (ICA) based on the EEGlab toolbox [33] was exploited to remove the artifacts related to muscle contraction, heart beating, and eye movement from recorded EEG data. The ICA components exhibiting a correlation higher than 0.4 with EOG signals were considered artifacts. After eliminating artifact-related components, EEG signals were reconstructed from the remaining components. To avoid any residual artifacts, the seven most frontal electrodes in rows Fp and AF besides the electrodes, TP9, P9, and P10 were excluded for further analysis (Fig. 1(A)). The remaining 53 electrodes were used for data processing. In order to enhance the spatial resolution of EEG signals, the surface Laplacian filter was applied to movement phase data [34]. The hand movement position data recorded via LeapMotion in the movement phase of each trial were upsampled to the sampling rate of 512 Hz to be equal in sample length to the corresponding recorded EEG data. All signal analysis was performed with MATLAB 2019b (The MathWorks, Inc.).

D. STATE-BASED APPRAOCH AND CLASSIFCATION

The state-based approach is composed of two steps: first, the discrete-state decoder determines the movement category (class) of the current test trial. Then, the corresponding regression model based on the predicted movement category of the test trial is employed for trajectory decoding. The key idea of the state-based approach is to train the continuous decoder (regressor) for each axis only with the trials featuring hand movement along that specific axis. For instance, the regressor model for the x-axis should only be trained on the trials with hand movement towards targets T1 and T3 in our task. The movements towards T2 or T4 do not produce hand displacement along the x-axis, so these data should only be used for training the y-axis regressor model. This approach will lead to better decoding performance along each axis compared to the conventional non state-based technique. In a center-out task with movement along orthogonal axes, the state-based decoder recognizes the axis of movement, so it does not produce unwanted displacement along the axis in which the movement does not happen. To implement a state-based decoding approach, one requires designing a discrete

state decoder that discriminates movements along the x-axis and y-axis. To this end, the trials featuring movement along the x-axis (reaching towards T1 or T3) and the trials with movement along the y-axis (reaching towards T2 or T4) were labeled as class 1 and class 2 respectively. Determining the axis in which the movement happens is of great importance for achieving competitive performance in the state-based technique. The performance of the whole method depends on correct state detection.

The discrete state-decoder was designed based on common spatial pattern (CSP) feature extraction and SVM classifier. As stated earlier, the feasibility of decoding direction from EEG data before movement onset/go cue has been confirmed in the literature [25], [27]. We considered a 500ms time window before the go cue for training the state decoder. In our analysis, this interval led to the best results. The CSP algorithm seeks to find a linear transformation that maximizes the variance of EEG signals from one class while minimizing the variance of signals of the other class at the same time. Let $\boldsymbol{X}\in\mathbb{R}^{T\times C}$ denote a recorded trial of multi-channel EEG data where T is the length of the trial and C is the number of channels. The CSP transformation matrix $\boldsymbol{W}_{csp}\in\mathbb{R}^{C\times 2m}$ can be considered as a spatial filter combining the recorded channels to construct a new data space $\boldsymbol{Z} = \boldsymbol{X}\boldsymbol{W}_{csp}$ offering optimal discrimination between power features of two classes. The columns of $\boldsymbol{W}_{csp}$ are denoted by $\boldsymbol{w}_j\in\mathbb{R}^C$. The CSP algorithm extremizes the following cost function:

$$J(\boldsymbol{w}) = \frac{\boldsymbol{w}^T\boldsymbol{\Sigma}_1\boldsymbol{w}}{\boldsymbol{w}^T\boldsymbol{\Sigma}_2\boldsymbol{w}} \tag{1}$$

where $\boldsymbol{\Sigma}_i \in \mathbb{R}^{C\times C}$ represents the average covariance matrix of trials belonging to class $i \in \{1, 2\}$. The covariance matrix estimator for each trial is:

$$\boldsymbol{S} = \frac{\boldsymbol{X}^T\boldsymbol{X}}{trace(\boldsymbol{X}^T\boldsymbol{X})} \tag{2}$$

where $trace(.)$ is the trace operator which sums diagonal elements of a square matrix. For each class, the average covariance matrix will be calculated based on the corresponding training data:

$$\boldsymbol{\Sigma}_i = \frac{1}{|\phi_i|}\sum\nolimits_{j\in\phi_i}\boldsymbol{S}_j \tag{3}$$

ϕ_i represents the set of trials belonging to class i and $|\phi_i|$ is its cardinality. The CSP optimization problem represented in equation (1) can be solved by addressing the following generalized eigenvalue problem [35], [36]:

$$\boldsymbol{\Sigma}_2^{-1}\boldsymbol{\Sigma}_1\boldsymbol{w} = \lambda\boldsymbol{w} \tag{4}$$

where the generalized eigenvalue and eigenvector are represented by λ and $\boldsymbol{w}$. The spatial filter $\boldsymbol{W}_{csp}$ consist of eigenvectors corresponding to m maximum and minimum eigenvalues. The CSP features used for training the classifier are the logarithm of the variance of projected signals. In this study, we assumed $m = 3$, so there were six CSP features for training the classifier.

To build and evaluate our algorithm, a 10-fold cross-validation scheme was employed. The training data folds were used to build the model including discrete state-decoder and continuous decoder. The test data fold was used for evaluating the performance of the trained model. In Section III, the reported results were computed based on the average of ten repetitions of 10-fold cross-validation with shuffling the order of trials.

E. CONTINUOUS-DECODER DESIGN

The continuous decoder was designed based on the Gaussian process regression (GPR) which is a nonparametric, kernel-based, probabilistic model. GPR provides the possibility of flexible models which are practical to work by using the Gaussian process (GP) framework. GP extends the concept of multivariate Gaussian distribution into infinite-dimensional space. In fact, the GP model defines a probability distribution over possible functions that fit a set of given observations, whereas multivariate Gaussian distributions are only defined over vectors. Formally, "*A Gaussian Process is a collection of random variables, any finite number of which have joint Gaussian distributions*" [37]. A GP is fully characterized by its mean function $m(x)$ and kernel (covariance) function $k(\boldsymbol{x}, \boldsymbol{x'})$:

$$g \sim \mathcal{GP}\left(m(\boldsymbol{x}), k\left(\boldsymbol{x}, \boldsymbol{x'}\right)\right) \tag{5}$$

correspondingly, it defines function g as a gaussian process with specific mean and covariance functions. Generally, a regression problem can be considered as a model $y = f(\boldsymbol{x})$ with a set of n training observations: $\boldsymbol{y} = [y_1, y_2, \ldots, y_n] \in \mathbb{R}^n$ and $\boldsymbol{X} = [\boldsymbol{x_1}, \boldsymbol{x_2}, \ldots, \boldsymbol{x_n}] \in \mathbb{R}^{d\times n}$. The dimension of feature space is denoted by d. To fit a GP model to unknown function f, the kernel function should be calculated among all possible combinations of training data resulting in the kernel matrix $\boldsymbol{K}$ defined as:

$$\boldsymbol{K} = K(\boldsymbol{X}, \boldsymbol{X}) = \begin{bmatrix} k(\boldsymbol{x_1}, \boldsymbol{x_1}) & \cdots & k(\boldsymbol{x_1}, \boldsymbol{x_n}) \\ \vdots & \ddots & \vdots \\ k(\boldsymbol{x_n}, \boldsymbol{x_1}) & \cdots & k(\boldsymbol{x_n}, \boldsymbol{x_n}) \end{bmatrix} \tag{6}$$

For the given training data and known mean and kernel function, the GP specifies a regular multivariate Gaussian distribution as $\mathbf{f} \sim \mathcal{N}(\boldsymbol{m}, \boldsymbol{K})$. It is common to normalize data before the processing, so the mean function is a constant zero vector. The choice of kernel determines the smoothness of the function. Theoretically, any positive definite function can be employed as a kernel function [37]. It defines the relationship between observations.

Given the training dataset, the GP method can make inferences about the function f governing the relation between input $\boldsymbol{x_i}$ and output y_i. This GP process can be used as a prior for Bayesian inference. It is necessary to compute the posterior distribution for a specific set of test cases given the training dataset to predict unseen test data. Assume that $\boldsymbol{X}_*$ is the set of test samples. The objective is to find the posterior distribution for test data which is denoted by $\mathbf{f}_*$ given the

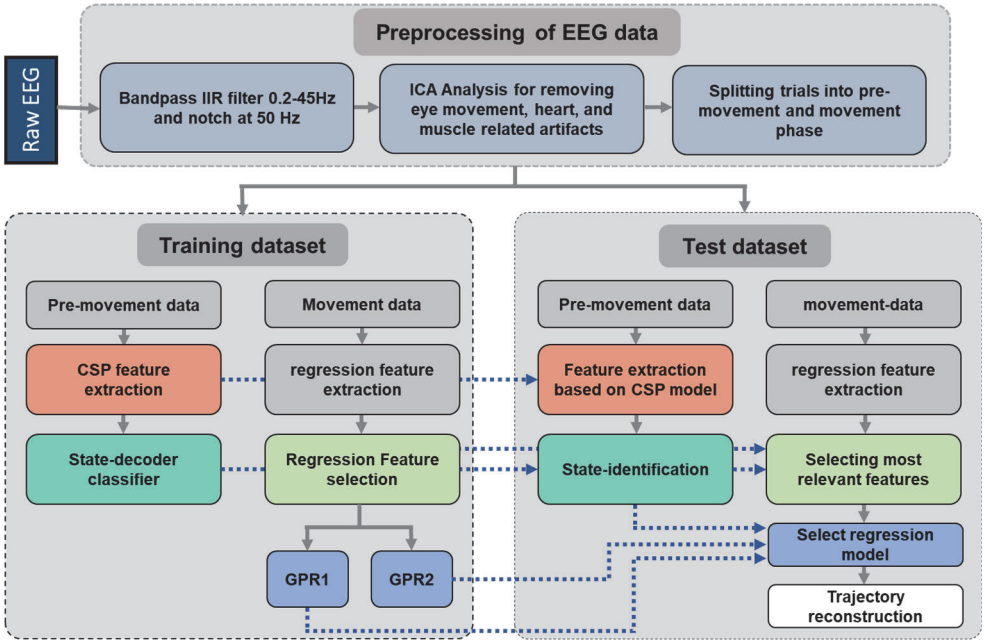

FIGURE 2. Schematic of the proposed state-based decoding pipeline. The solid grey lines show the flow of data. The dashed blue lines represent the flow of trained models.

training data (i.e. $\mathbf{f}_*|\mathbf{f}$). The derivation of the posterior is rather straightforward based on the properties of Gaussian distributions and can be found in [38].

$$f_* \,|f \sim \mathcal{N}\left(\boldsymbol{K}_*\boldsymbol{K}^{-1}\boldsymbol{y}, \boldsymbol{K}_{**}\boldsymbol{K}^{-1}\boldsymbol{K}_*^{\boldsymbol{T}}\right) \tag{7}$$

where $\mathbf{K}_* = K(\boldsymbol{X}, \boldsymbol{X}_*)$ and $\mathbf{K}_{**} = K(\boldsymbol{X}_*, \boldsymbol{X}_*)$ represent kernel matrix for the training-test set and test set respectively. Matrix transposition operation is denoted by superscript T. The best estimate for regression results is the mean of the distribution presented in equation (7):

$$\hat{f} = \boldsymbol{K}_*\boldsymbol{K}^{-1}\boldsymbol{y} \tag{8}$$

The above formulation is derived for a noise-free situation. In real-world applications, observations are contaminated with noise. The most common assumption is to consider independent additive white Gaussian noise in the outputs i.e. $y = f(\boldsymbol{x}) + \epsilon$, where $\epsilon \sim \mathcal{N}(0, \sigma_\epsilon^2)$. This assumption can be easily incorporated into the GPR formulation. The covariance function of noisy observations is the sum of signal covariance and noise covariance. Considering the noise in the equation prevents the GP model from overfitting on training data. The formulation for regression in presence of noisy observation is [38]:

$$\hat{f} = \boldsymbol{K}_*(\boldsymbol{K} + \sigma_\epsilon^2\boldsymbol{I})^{-1}\boldsymbol{y} \tag{9}$$

In this study, the squared exponential (SE) kernel was used for modeling the hand movements from EEG features. This kernel is infinitely differentiable and smooth which makes it a sensible choice for a broad range of applications. SE kernel is define as [38]:

$$k\left(\boldsymbol{x}, \boldsymbol{x}'\right) = \sigma_f^2 exp\left(-\frac{\left\|\boldsymbol{x} - \boldsymbol{x}'\right\|^2}{2l^2}\right) \tag{10}$$

where length-scale l and signal variance σ_f^2 are two hyperparameters of the kernel.

The common practice for estimating kernel hyperparameters is to optimize the marginal loglikelihood function based on its partial derivatives. The mathematical formulation for the loglikelihood function and hyperparameters optimization problem can be represented as [38]:

$$\hat{\boldsymbol{\theta}} = \underset{\boldsymbol{\theta}}{argmax}\left(\log p(\boldsymbol{y}|\boldsymbol{X}, \boldsymbol{\theta})\right) \tag{11}$$

$$\log p\left(\boldsymbol{y} \mid \boldsymbol{X}, \boldsymbol{\theta}\right) = -\frac{1}{2}y^T\boldsymbol{K}^{-1}\boldsymbol{y} - \frac{1}{2}\log|\boldsymbol{K}| - \frac{n}{2}\log(2\pi) \tag{12}$$

the kernel hyperparameters are denoted by vector $\boldsymbol{\theta} = [l, \sigma_f]$. In this study, the quasi-newton optimizer was used for kernel hyperparameters optimization. The additive noise variance σ_ϵ^2 was optimized via grid search on the training dataset. To evaluate the performance of the continuous decoding method, the Pearson correlation coefficient between reconstructed trajectory and actual movement has been calculated:

$$r = \frac{\sum_{t=1}^{T}(f(t) - \bar{f})(\hat{f}(t) - \bar{f})}{\sqrt{\sum_{t=1}^{T}(f(t) - \bar{f})^2}\sqrt{\sum_{t=1}^{T}(\hat{f}(t) - \bar{f})^2}} \tag{13}$$

where $f(t)$ and $\hat{f}(t)$ denote the actual and reconstructed trajectories at time t, respectively. The signals are T samples

long. $\bar{f}$ and $\hat{\bar{f}}$ indicate the sample mean of actual movement and reconstructed movement respectively.

F. FEATURES EXTRACTION AND FEATURES SELECTION

Numerous studies have reported successful decoding of upper-limb movement based on amplitude features extracted from EEG recordings. Early works by Waldert [22] and Bradbery [16] mainly indicated that features extracted from low-delta activities convey discriminative information about hand kinematics. The role of band-power features from mu, beta, and gamma frequency bands was later on confirmed in motion trajectory perdition by Korik et al. [18]. In this work, the amplitude features were extracted from 53 EEG channels in movement intervals for constructing the continuous-decoder model. The EEG data of movement interval were first filtered into six frequency bands: δ(0.2-4 Hz), θ(4-8 Hz), α(8-14 Hz), β1(14-20 Hz), β2 (20-30 Hz), and γ(30-45 Hz) via zeros phase, fourth order Butterworth filter. Then, the signals were rectified and smoothed using a low-pass, fourth order Butterworth filter with cutoff frequency at 1 Hz. This operation extracted the envelope of signals at six aforementioned frequency bands. The features were then normalized and downsampled to 8 Hz. Envelope features only include low-frequency content due to smoothing process. Hence, the process of downsampling the features helps reduce computational burden and processing time. The movement data were also downsampled to 8 Hz accordingly. In addition to the features corresponding to the present time sample, four time lags of the features were added to the feature vector (i.e. lag 0, −125ms, −250ms, −375ms and −500ms). In other words, to estimate the movement at a specific time t, we employed the features extracted at time sample t and four previous time samples. Since the signals were downsampled to 8 Hz, each time lag is equal to 125ms. In summary, the feature space includes 53∗6∗5=1590 features. In order to find the most relevant features to the hand motion, the mutual information (MI) measure has been employed. MI quantifies the amount of information obtained about one random variable by observing the other random variable [39]. For two random variables X and Y, MI is formulated as:

$$I(X,Y) = \sum_{i,j} P(X=x_i, Y=y_j) log\left(\frac{P(X=x_i, Y=y_j)}{P(X=x_i)P(Y=y_j)}\right) \quad (14)$$

MI quantity between extracted features and hand movement signals along each axis was calculated. The features were then ranked based on the highest MI and used for regressor training. The number of regression features was optimized separately for each subject. The optimum number of regression features was in the range of 50-200 features for each subject. In a nutshell, the whole methodology of target detection and trajectory reconstruction for the standard center-out task with four orthogonal directions can be summarized as follows: first, the discrete state-detector based on CSP feature extraction and SVM classifier is built using pre-movement data of training dataset. Additionally, two GPR models, one for decoding movement along the x-axis and another for decoding movement along the y-axis, are trained based on the most relevant envelope features extracted from movement interval data. For each test trial, the state-detector first decides whether the trial belongs to class 1 or class 2 by analyzing its pre-movement interval. Then, the corresponding GPR model is employed to reconstruct the motion trajectory from movement phase data. The proposed methodology is summarized in Fig. 2. The results of applying the proposed method to the four-target task are reported in the first part of Section III.

G. GENERALIZATION OF BINARY CLASSIFICATION FOR RANDOM TARGET DETECTION

The center-out task has been generalized with additional random targets to assess the competence of the proposed state-based method. As stated earlier, the number of random targets was limited, so the model was not trained on them. They were just used for testing the generalizability. To incorporate the random targets into the methodology, the algorithm first requires to identify whether the test trial at hand belongs to class 1, class 2, or random targets which are labeled as class 3. Consequently, the binary state-detector described in Section II-D should be generalized to identify three classes. This issue can be addressed by applying new boundaries on the score space of the trained binary classifier.

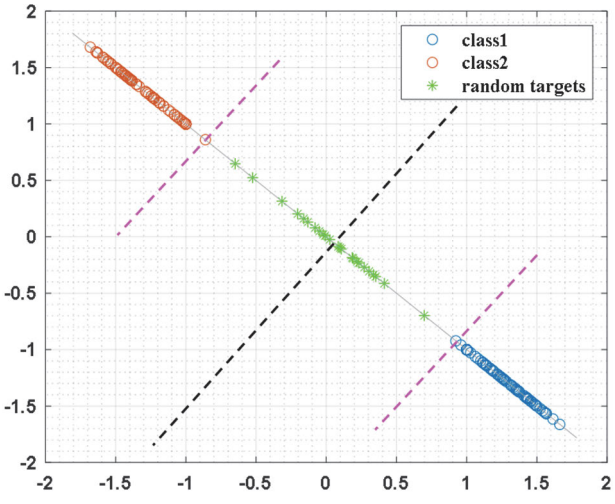

FIGURE 3. The score space of binary SVM classifier with RBF kernel trained on subject 6 data. The blue and red circles denote the class 1 and class 2 training trials. The score values of random targets trials -projected with W_{csp} and classified with trained binary classifier- are depicted by green stars. The original boundary of the binary classifier is illustrated by the dashed black line. Two new boundaries for three-class discrimination are denoted by the dashed magenta line. The one-dimensional score space is illustrated diagonally for better visual presentation.

The score space of the binary SVM classifier which has been trained on a training dataset of the binary problem (class 1 vs. class 2 data) is illustrated in Fig. 3 (a representative example from the subject 6 dataset). The classifier projects the input features into a score space where the

samples show the most discrimination. Actually, the classifier makes decisions based on the value of scores. The binary classification is performed based on the boundary denoted by the dashed black line in Fig 3 which is orthogonal to the score space line. The feature extraction for class 1 and class 2 data is based on the CSP technique which maximizes the variance of one class while minimizing the variance of the other class. The class 3 data belong to none of class 1 or class 2 data. When the class 3 data are transformed using $\boldsymbol{W}_{csp}$ trained on class 1 and class 2 data, the results differ from class 1 and class 2 projected data. Hence, in the score space of the trained binary classifier, the random target trials happen between the score values of the two classes. They are distributed near the binary classifier boundary. The trials belonging to random targets are depicted with green stars in Fig 3.

To infer three-class discrimination from this problem, two boundaries are required to be determined based on training data samples of class 1 and class 2. Two new boundaries are defined based on the score values of class 1 and class 2 training samples which are nearest to the binary discrimination boundary (dashed black line in Fig. 3). The new boundaries are depicted in magenta in Fig 3. If the score value of a test trial occurs between these two lines, the trial belongs to class 3. The classification performance of the three-class scenario is reported based on the 10 × 10-fold cross-validation scheme in Section III-B. The nine training folds of class 1 and class 2 data have been used for calculating CSP transformation ($\boldsymbol{W}_{csp}$) and training the SVM model. Then, the two boundaries for three-class discrimination were computed. Next, the test fold data of class 1, class 2, and the whole random target trials were classified using the three-class state-based decoder. Therefore, the whole 24 random trials were classified 100 times during cross-validation, and the detection accuracy rates were reported for each subject. In this study, the SVM classifier with RBF kernel achieved the best true positive rate for detecting random targets and also, the best accuracy in three-class discrimination scenario compared to linear SVM, linear discriminant analysis (LDA), and quadratic discriminant analysis (QDA) (see Figure S1 in supplementary materials). Hence, only the SVM classifier with RBF kernel was used for the discrete-state detection throughout the paper. It should be noted that the source code of the proposed method written in MATLAB is available at GitHub.[1]

III. RESULTS

The results of the study are divided into four parts. The first part is dedicated to applying the proposed method to a standard center-out task with four orthogonal targets. The results of the generalization of the task with random targets are summarized in the second part. The third part includes surrogate data analysis and investigations on EEG sub-band performance. The comparison between the state-based and the conventional approach is offered in the fourth part.

[1](https://github.com/moosahosseini/EEG_state_based).

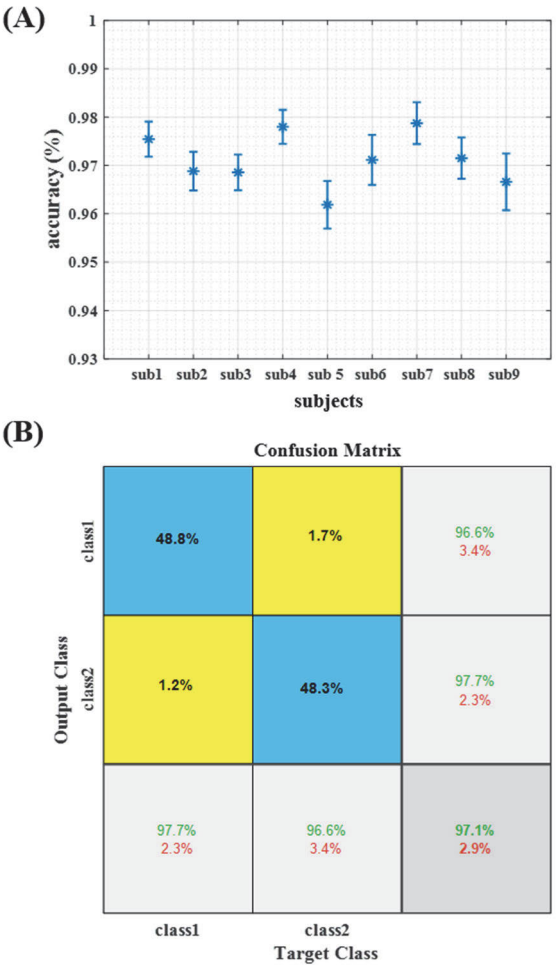

FIGURE 4. (A) The accuracy of binary classification (mean±SE) for each subject based on 10×10-fold cross-validation results. (B) The confusion matrix which was calculated based on the results from all subjects.

A. CENTER-OUT TASK WITH FOUR ORTHOGONAL TARGETS

The state-based scheme consists of two parts. The first is the state detector which determines the axis on which the movement happens. The second part is continuous trajectory decoding along the axis of movement. As we stated earlier in part II-D, the state detector is based on CSP features extracted from pre-movement SCP signals and binary SVM classification. In the standard center-out task with four principal targets, the state-detector discriminates between class 1 (T1 or T3) and class 2 (T2 or T4). The binary classification accuracy results for nine subjects are presented in Fig 4. The classification accuracy (mean±SE) is reported based on a 10 × 10-fold cross-validation scheme for each subject (Fig. 4(A)). The total performance of the binary decoder is also assessed through the calculation of the confusion matrix over all subjects depicted in Fig. 4(B). The proposed method has obtained an average accuracy of 97.1% over all participants.

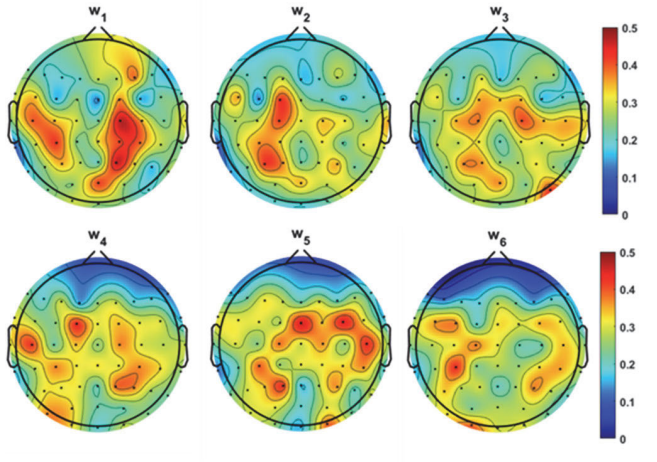

FIGURE 5. The contribution of recording channels in CSP feature extraction. The Topoplot graphs display the average of absolute CSP weight vectors over all subjects.

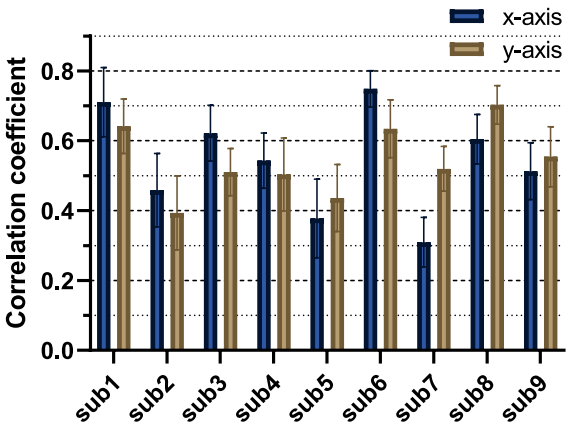

FIGURE 6. Regression results of the proposed method on principal targets trajectories for each subject in terms of correlation coefficient (mean±SD).

The weight vectors (i.e. $\boldsymbol{w}_j$ (j = 1, 2, . . . , 6)) of CSP algorithm can be considered as spatial filters combining recording channels to build a new channel space with maximum discrimination between variance features of two classes. Fig. 5 displays the contribution of each recording channel in binary discrimination by calculating the average of absolute values of six CSP weight vectors over all subjects. The results show that frontoparietal and central areas are mostly involved in extracting features for classification.

After determining the label of the test trials, the corresponding continuous decoder is employed to reconstruct the movement trajectory. Two GPR models have been built on training data for decoding movement along the x-axis and y-axis separately. In other words, the GPR1 and GPR2 models were trained on trials belonging to class 1 and class 2 for decoding movement along the x-axis and y-axis respectively (pipeline presented in Fig. 2). Fig. 6 summarizes regression results of the proposed state-based algorithm on principal targets for each subject. The performance of each model is reported separately in terms of the Pearson correlation coefficient. The average correlation coefficient of both models over all subjects is 0.54±0.12. A representative example of reconstructed trajectory with the proposed method along the x-axis and y-axis is provided in Fig. 7.

B. GENERALIZED CENTER-OUT TASK WITH RANDOM TARGETS

Here we presented the results of detecting and continuously decoding the trajectories of random targets in the generalized center-out task. In Section II-G, we described the technique for detecting the random targets based on the classifier trained on two classes of principal targets. The performance of detecting random target trials is reported based on the true positive rate which is defined as the percentage of truly detected random targets to all random targets. Fig. 8(A) summarizes the true positive rate (sensitivity) of detecting random

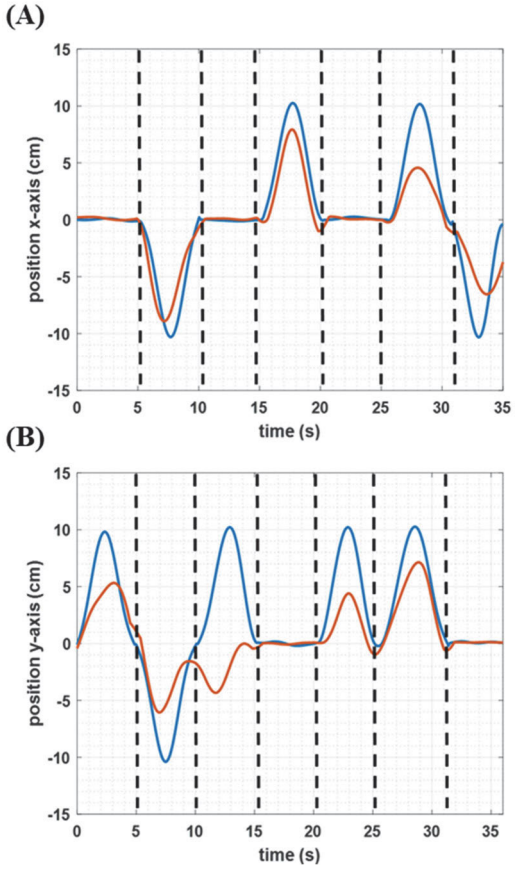

FIGURE 7. A representative example of reconstructed trajectory with proposed method on data from subject 6. (A) Reconstruction along x-axis. (B) Reconstruction along y-axis. The dashed lines represent the beginning of test trials. The classifier switches between classes and select proper regression model based on pre-movement data.

targets for each subject. The confusion matrix calculated for three-class discrimination of test trials in the generalized task is presented in Fig. 8(B). The total accuracy of classification reached 87.3% in the generalized task with three classes

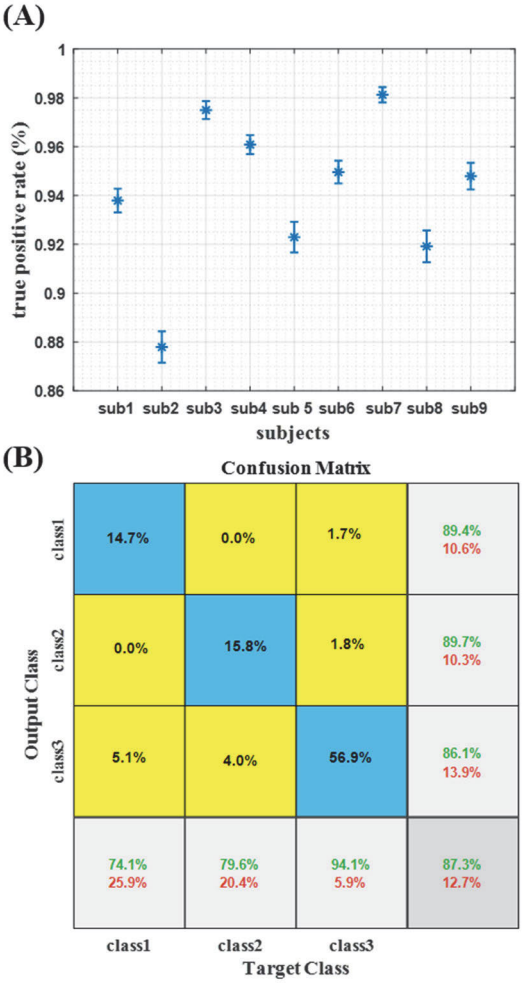

FIGURE 8. (A) True positive rate (sensitivity) of detecting random targets for all subjects (mean±SE). (B) The confusion matrix for three-class discrimination was calculated.

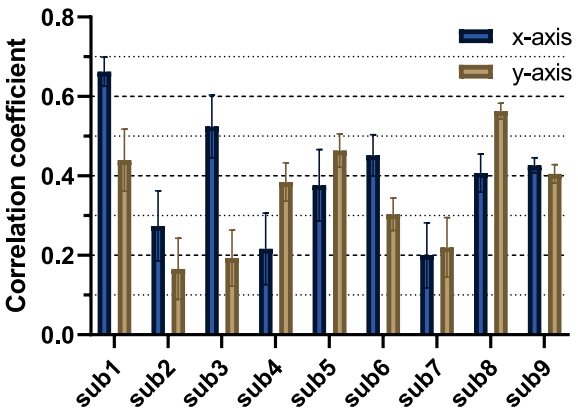

FIGURE 9. Regression results of the proposed method on random targets for each subject in terms of correlation coefficient (mean±SD).

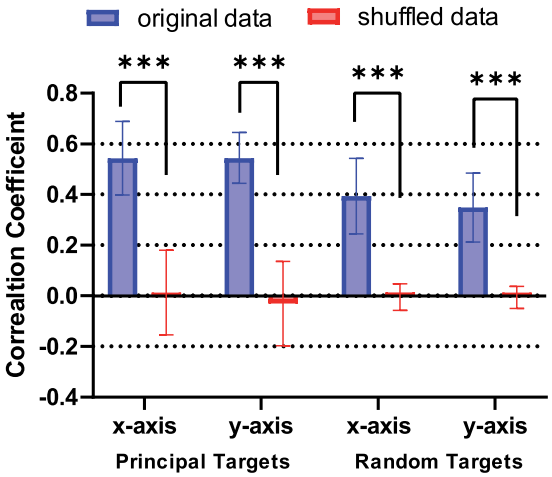

FIGURE 10. Investigating the statistical significance of the continuous decoding method. The chance level was calculated based on a shuffled surrogate data model. Each bar represents the Pearson correlation coefficient (mean ± SD) which is calculated based on 10×10-fold crossvalidation and then averaged over all nine subjects(***: p-value<0.001, Wilcoxon rank-sum test).

of test trials. The objective of this section is to assess the generalizability of the center-out task trained on orthogonal directions for identifying trials featuring out-of-axis movements. Hence, the results are focused on detecting random targets and estimating corresponding trajectories.

After identifying the random target trials, both trained GPR models have been exploited for trajectory reconstruction along the x-axis and y-axis simultaneously. The results of random target trajectory reconstruction along the x-axis and y-axis are depicted in Fig. 9.

C. INSPECTING STATISTICAL SIGNIFICANCE AND THE PERFORMANCE OF EEG SUB-BANDS

In order to investigate the statistical significance of the proposed method, surrogate datasets were generated by randomly shuffling the order of brain features [17], [40]. Then, the proposed method was employed to estimate hand kinematics from the surrogate datasets of each subject. Our findings suggest that the hand trajectories based on original datasets were decoded significantly above chance level for both principal target and random targets along the x-axis and y-axis (Wilcoxon rank-sum test, $p<0.001$). The results of the statistical test are portrayed in Fig. 10.

The capability of individual EEG sub-bands was examined in continuous trajectory decoding using the proposed method. For this sake, the EEG activity of six sub-bands defined in Section II was separately fed into the proposed continuous decoder. The feature extraction and feature selection were done on each sub-band accordingly and the results of the regression were summarized in Table 1. The features extracted from alpha and delta bands achieved better results compared to other sub-band. Table 1 confirms that using single-band features would lead to inferior results, especially for random target reconstruction.

D. STATE-BASED VERSUS CONVENTIONAL APPROACH

We claimed that exploiting the state-based approach would lead to a better continuous decoder model compared to the

TABLE 1. The trajectory reconstruction performance of individual EEG sub-bands and the proposed approach based on extracting features from all six sub-bands. The correlation coefficients of decoding principal targets and random targets trajectories-averaged over all subjects- are reported separately based on 10 × 10-fold CV.

Sub-Band	Principal targets	Random targets
δ	0.32	0.12
θ	0.21	0.03
α	0.45	0.11
$\beta 1$	0.23	0.02
$\beta 2$	0.25	0.12
γ	0.22	0.05
All	<u>0.54</u>	<u>0.37</u>

The best approach is underlined for each dataset.

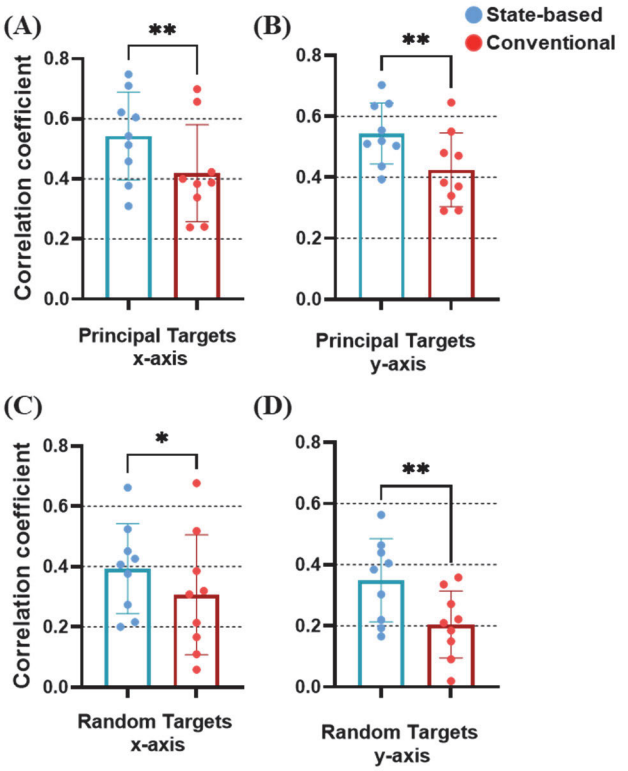

FIGURE 11. Comparing the continuous decoding performance of the proposed state-based method to the conventional approach. Each bar represents the correlation coefficient (mean±SD) averaged over all subjects. The dots correspond to the average results for each subject. (A) Comparing reconstruction performance of principal targets over the x-axis. (B) Comparing reconstruction performance of principal targets over the y-axis. (C) Comparing reconstruction performance of random targets over the x-axis. (D) Comparing reconstruction performance of random targets over the y-axis. (*: p-value<0.05, **: p-value<0.01, Wilcoxon matched-pairs signed-rank test).

conventional approach. The conventional approach is to build the model on all training data without separating trials based on the type of movement. Hence, the regressor of the x-axis, for instance, is trained on all training trials where the subject performed movement towards all four orthogonal targets. Two of the targets do not require movement along the x-axis (T2 and T4). Using these trials for training the x-axis regressor would weaken the continuous decoding model because the regressors are not capable of modeling stillness. The story is the same for calculating the y-axis regressor in the conventional approach. In the state-based approach, the regressor of each axis is only trained on the trials featuring hand movement along that axis. This method requires state detection which has been explained throughout the study. In this section, the results of the proposed state-based method are compared to the conventional method. For implementing the conventional approach, we eliminated the state-detection block from our methodology and built the GPR models on all training data without separating them based on movement along the x-axis or y-axis. The preprocessing, feature extraction and feature selection remained the same. Fig 11 compares the average correlation coefficient results of reconstructing principal targets and random targets using state-based and conventional methods. The state-based approach achieved superior performance for both estimating principal targets and random targets trajectories along each axis. To validate the statistical significance of the state-based method against the conventional approach, a Wilcoxon matched-pairs signed rank test was applied to the data presented in Fig. 11. The statistical test outcome confirms that the continuous decoding models based on the state-based approach provide superior results compared to the conventional method ($p<0.05$).

The conventional approach was also implemented based on MLR [16], ridge [41], Kalman [42], SVR [43], and PLS [44] decoders. The proposed method outperformed all these conventional implementations. The detailed subject to subject results are presented in supplementary materials (Tables S1 and S2).

IV. DISCUSSION

Although the EEG-based BCI systems aiming for hand motion trajectory reconstruction have gained considerable attention due to their budget-friendly implementation and minimal health issues, the inferior performance compared to invasive BCIs confines their real-world applications. In this work, a state-based approach has been proposed to enhance the prediction of hand movements based on EEG recordings. The state-based decoding paradigm has been considered in several invasive studies. Aggarwal et al. [28] implemented a state-based model with a linear discriminant classifier and Kalman filter for distinguishing periods of posture and hand movements based on neural ensemble and LFP activities recorded from the primary motor and pre-motor cortex of two rhesus monkeys. Bundy et al. [29] designed a hierarchical partial least square (PLS) method with logistic regression as a discrete decoder for enhancing continuous estimation

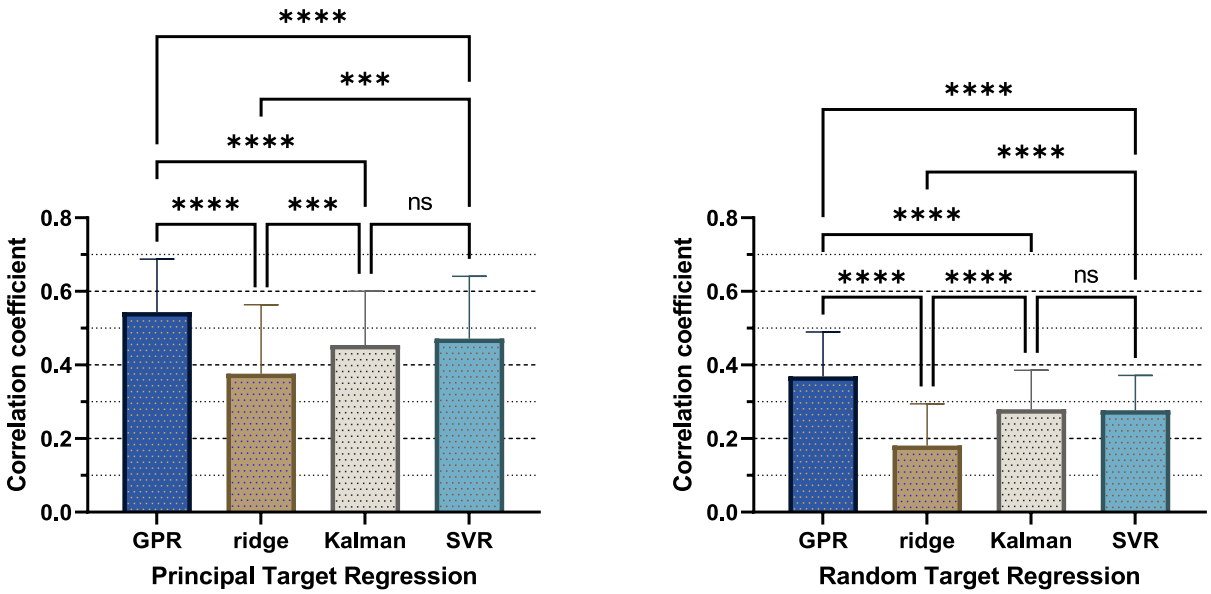

FIGURE 12. Comparing results of proposed GPR with ridge, Kalman, and SVR methods on principal target and random target trajectory reconstruction. The bars represent the correlation coefficient (mean±SD) of each method averaged over all subjects. (A) Results for principal target decoding. (B) Results for random target decoding. (ns: not significant, ***: p-value<0.001, ****: p-value<0.0001, Friedman test with FDR correction for multiple comparisons).

of reaching movement in a center-out task using electrocorticographic signals in human subjects. Ahmadi et al. [45] proposed a method combining filter-bank CSP and PLS regression for improving continuous force decoding from LFP signals acquired from rats performing a key-pressing task.

As far as we know, this is the first study proposing a state-based decoding paradigm for hand motion trajectory prediction from an EEG center-out-reaching task generalized with random targets. In order to distinguish between states which have been defined as movements along the x-axis and y-axis, the CSP features extracted from pre-movement data have been used. Identifying the movement intention from pre-movement brain activities increases the practical applicability of BCI systems [27]. The continuous decoding of hand motions based on features extracted from movement interval was done using the GPR framework which is a non-parametric flexible kernel method [46]. The augmentation of the task with random targets allows for evaluating the performance of the proposed method on a new type of data on which the model has never been trained.

The proposed discrete decoder based on the CSP method combines EEG channels to build a new signal space with maximum discrimination between variance features of two classes. Fig. 5 demonstrates the contribution of channels by depicting the average absolute value of CSP weight vectors $\boldsymbol{w}_j$ over all subjects. The channels overlay central, centroparietal, and frontocentral regions such as C1, C2, CP3, CP2, P2, P3, FCz, and FC1 represent the most contribution, especially in the first three weight vectors. Inspecting topoplots from $\boldsymbol{w}_4$, $\boldsymbol{w}_5$ and $\boldsymbol{w}_6$ emphasizes the apparent role of frontocentral and frontoparietal channels in state classification as well. The results are in agreement with a study by Lew et al. [26] which found discriminative patterns involving central and frontoparietal areas during reaching tasks for both able-bodied and stroke patients. A study by Contreras-Vidal et al. [47] on visuomotor adaptation in an EEG center-out task has also shown the involvement of frontoparietal regions in healthy participants. The association of parietal EEG components with intended movement direction was also investigated in [48].

One of the key aspects of the proposed method is the use of GPR for continuous decoding. This method is capable of alleviating the effect of noise in the data by modeling it as an additive white Gaussian element. To evaluate the effectiveness of the proposed continuous decoder in the context of regression analysis, we substituted the GPR model with three other well-known regression methods in the proposed methodology. Fig. 12 compares the performance of the proposed method based on GPR decoding to ridge regression [41], Kalman filter [42], and support vector regression (SVR) [43] with RBF kernel on both principal and random targets. The ridge regression and Kalman filter are two linear methods that are very popular in movement decoding [19], [49], [50]. The SVR method is a nonparametric, kernel-based technique based on the idea of support vector machine (SVM) analysis. The performance of the proposed method against the other three methods has been assessed from the statistical point of view by applying a one-way repeated, non-parametric Friedman test followed by FDR correction for multiple comparisons [54]. The statistical test was applied to the results of a 10×10-fold cross-validation data of all subjects (Fig. 12).

TABLE 2. Comparison to some relevant trajectory decoding studies of hand kinematics based on EEG recordings.

Authors	Number of subjects	Movement Task	Feature/Technique	Results (correlation coefficient)	Reference
Bradberry et al. 2010	five	3D Center-out	MLR[a]	0.30	[16]
Kim et al. 2015	ten	Drawing trajectory	MLR, KRR[b]	0.46	[51]
Korik et al 2018	twelve	3D Center-out	MLR	0.4	[18]
Mondini et al 2020	ten	Pursuit tracking task	PLS[c] + Kalman	0.32	[19]
Kobler et al. 2020	fifteen	Pursuit tracking task	UKF[d]	0.49	[52]
Jeong et al. 2020	fifteen	3D Center-out	MDCBN[e]	0.47	[53]
Hosseini et al. 2022	seven	2D Center-out	Connectivity + MLR	0.42	[20]
Wang et al. 2022	eight	2D Center-out	Ensemble decoder	0.29	[21]
Present study	nine	2D Center-out	State-based GPR	0.54	

[a]Multiple Linear Regression, [b]Kernel Ridge Regression, [c]Partial Least Squares, [d]Unscented Kalman Filter, [e] Multi-Directional CNN-BiLSTM Network.

The proposed method outperformed the other methods both in decoding principal targets and random targets trajectories with statistical significance ($p<0.0001$).

It is necessary to compare our results to some related works. Bradberry et al. first verified that the information content of EEG recordings is sufficient for decoding hand trajectories during the center-out reaching task [16]. Numerous studies have been conducted to improve the results of hand movement trajectory prediction based on EEG data since the work by Bradberry. Table 2 summarizes some related works to EEG-based upper-limb motion decoding. The most common experimental paradigms were 2D and 3D center-out tasks. The pursuit tracking task was also considered in some studies [19], [52]. Although early studies employed linear decoding models, non-linear methods such as unscented Kalman filter (UKF) and neural networks have attracted considerable attention recently. [21], [52]. Decoding upper limb movement based on non-invasive recordings has progressed noticeably during the last decade. However, the results have to be improved further for rehabilitation purposes. Invasive studies appear to still have the edge over non-invasive research in terms of motion reconstruction accuracy [8], [50].

Despite significant improvement upon the conventional approach and some well-known regression algorithms, the conducted study is not without caveats. First, the center-out task used in this work was limited to four orthogonal directions. It is worthwhile to study the trajectory reconstruction performance when the number of training directions increases. Second, the number of random targets was limited in the study. Hence, they were only used for testing the generalizability of the proposed method. A study with a large number of random targets is required to investigate whether using random targets in training the model enhances the overall decoding capabilities. Third, our participants were limited to male subjects at young adulthood age. It is necessary to conduct the experiment with larger number of subjects including both male and female participants at different ages. Moreover, the whole analysis of this work was done offline. An online extension of the study would be beneficial since the real-world applications of BCIs require real-time data processing.

V. CONCLUSION

In this study, the capability of discrete state decoding based on pre-movement data was employed to enhance the performance of reconstructing hand movement trajectories in an EEG center-out task. Our proposed method combines a discrete state decoder based on the CSP algorithm with GPR continuous decoders. To evaluate the generalizability of the decoding model, the standard four-target center-out task was augmented with random targets. Our findings revealed that the random target trajectories can be decoded based on the training dataset including four orthogonal directions. Comparing the results of the proposed state-based method with the conventional method showed that the proposed method improves the trajectory prediction performance on both principal targets and random targets. The proposed methodology could be employed for developing new generations of BCIs with generalization capability which is key for real-world applications.

REFERENCES

[1] D. McFarland and J. Wolpaw, "EEG-based brain–computer interfaces," *Current Opinion Biomed. Eng.*, vol. 4, pp. 194–200, Dec. 2017, doi: 10.1016/j.cobme.2017.11.004.

[2] R. P. N. Rao, *Brain-Computer Interfacing: An Introduction*. Cambridge, U.K.: Cambridge Univ. Press, 2013.

[3] B. Blankertz, M. Tangermann, C. Vidaurre, S. Fazli, C. Sannelli, S. Haufe, C. Maeder, L. Ramsey, I. Sturm, G. Curio, and K.-R. Müller, "The Berlin brain–computer interface: Non-medical uses of BCI technology," *Frontiers Neurosci.*, vol. 4, pp. 1–17, Dec. 2010, doi: 10.3389/fnins.2010.00198.

[4] A. Myrden and T. Chau, "A passive EEG-BCI for single-trial detection of changes in mental state," *IEEE Trans. Neural Syst. Rehabil. Eng.*, vol. 25, no. 4, pp. 345–356, Apr. 2017, doi: 10.1109/TNSRE.2016.2641956.

[5] K. K. Ang and C. Guan, "Brain–computer interface for neurorehabilitation of upper limb after stroke," *Proc. IEEE*, vol. 103, no. 6, pp. 944–953, Jun. 2015, doi: 10.1109/JPROC.2015.2415800.
[6] M. Ahn, M. Lee, J. Choi, and S. C. Jun, "A review of brain-computer interface games and an opinion survey from researchers, developers and users," *Sensors*, vol. 14, no. 8, pp. 14601–14633, Aug. 2014, doi: 10.3390/s140814601.
[7] A. P. Georgopoulos, A. B. Schwartz, and R. E. Kettner, "Neuronal population coding of movement direction," *Science*, vol. 233, no. 4771, pp. 1416–1419, 1986.
[8] D. M. Taylor, S. I. H. Tillery, and A. B. Schwartz, "Direct cortical control of 3D neuroprosthetic devices," *Science*, vol. 296, no. 5574, pp. 1829–1832, 2002, doi: 10.1126/science.1070291.
[9] L. R. Hochberg, M. D. Serruya, G. M. Friehs, J. A. Mukand, M. Saleh, A. H. Caplan, A. Branner, D. Chen, R. D. Penn, and J. P. Donoghue, "Neuronal ensemble control of prosthetic devices by a human with tetraplegia," *Nature*, vol. 442, no. 7099, pp. 164–171, Jul. 2006, doi: 10.1038/nature04970.
[10] L. R. Hochberg, D. Bacher, B. Jarosiewicz, N. Y. Masse, J. D. Simeral, J. Vogel, S. Haddadin, J. Liu, S. S. Cash, P. van der Smagt, and J. P. Donoghue, "Reach and grasp by people with tetraplegia using a neurally controlled robotic arm," *Nature*, vol. 485, no. 7398, pp. 372–375, May 2012, doi: 10.1038/nature11076.
[11] S.-P. Kim, J. D. Simeral, L. R. Hochberg, J. P. Donoghue, and M. J. Black, "Neural control of computer cursor velocity by decoding motor cortical spiking activity in humans with tetraplegia," *J. Neural Eng.*, vol. 5, no. 4, pp. 455–476, Dec. 2008, doi: 10.1088/1741-2560/5/4/010.
[12] R. D. Flint, E. W. Lindberg, L. R. Jordan, L. E. Miller, and M. W. Slutzky, "Accurate decoding of reaching movements from field potentials in the absence of spikes," *J. Neural Eng.*, vol. 9, no. 4, Aug. 2012, Art. no. 046006, doi: 10.1088/1741-2560/9/4/046006.
[13] B. Farrokhi and A. Erfanian, "A state-based probabilistic method for decoding hand position during movement from ECoG signals in non-human primate," *J. Neural Eng.*, vol. 17, no. 2, May 2020, Art. no. 026042.
[14] C. A. Chestek, V. Gilja, P. Nuyujukian, J. D. Foster, J. M. Fan, M. T. Kaufman, M. M. Churchland, Z. Rivera-Alvidrez, J. P. Cunningham, S. I. Ryu, and K. V. Shenoy, "Long-term stability of neural prosthetic control signals from silicon cortical arrays in rhesus macaque motor cortex," *J. Neural Eng.*, vol. 8, no. 4, Aug. 2011, Art. no. 045005, doi: 10.1088/1741-2560/8/4/045005.
[15] S. Waldert, "Invasive vs. non-invasive neuronal signals for brain-machine interfaces: Will one prevail?" *Frontiers Neurosci.*, vol. 10, p. 295, Jun. 2016, doi: 10.3389/fnins.2016.00295.
[16] T. J. Bradberry, R. J. Gentili, and J. L. Contreras-Vidal, "Reconstructing three-dimensional hand movements from noninvasive electroencephalographic signals," *J. Neurosci.*, vol. 30, no. 9, pp. 3432–3437, Mar. 2010, doi: 10.1523/jneurosci.6107-09.2010.
[17] A. Úbeda, J. M. Azorín, R. Chavarriaga, and J. D. R. Millán, "Classification of upper limb center-out reaching tasks by means of EEG-based continuous decoding techniques," *J. NeuroEng. Rehabil.*, vol. 14, no. 1, pp. 1–14, Dec. 2017, doi: 10.1186/s12984-017-0219-0.
[18] A. Korik, R. Sosnik, N. Siddique, and D. Coyle, "Decoding imagined 3D hand movement trajectories from EEG: Evidence to support the use of mu, beta, and low gamma oscillations," *Frontiers Neurosci.*, vol. 12, p. 130, Mar. 2018, doi: 10.3389/fnins.2018.00130.
[19] V. Mondini, R. J. Kobler, A. I. Sburlea, and G. R. Müller-Putz, "Continuous low-frequency EEG decoding of arm movement for closed-loop, natural control of a robotic arm," *J. Neural Eng.*, vol. 17, no. 4, Aug. 2020, Art. no. 046031, doi: 10.1088/1741-2552/aba6f7.
[20] S. M. Hosseini and V. Shalchyan, "Continuous decoding of hand movement from EEG signals using phase-based connectivity features," *Frontiers Hum. Neurosci.*, vol. 16, p. 408, Jun. 2022, doi: 10.3389/fnhum.2022.901285.
[21] J. Wang, L. Bi, W. Fei, and K. Tian, "EEG-based continuous hand movement decoding using improved center-out paradigm," *IEEE Trans. Neural Syst. Rehabil. Eng.*, vol. 30, pp. 2845–2855, 2022, doi: 10.1109/TNSRE.2022.3211276.
[22] S. Waldert, H. Preissl, E. Demandt, C. Braun, N. Birbaumer, A. Aertsen, and C. Mehring, "Hand movement direction decoded from MEG and EEG," *J. Neurosci.*, vol. 28, no. 4, pp. 1000–1008, 2008, doi: 10.1523/JNEUROSCI.5171-07.2008.
[23] N. Robinson, C. Guan, A. P. Vinod, K. K. Ang, and K. P. Tee, "Multi-class EEG classification of voluntary hand movement directions," *J. Neural Eng.*, vol. 10, no. 5, Oct. 2013, Art. no. 056018, doi: 10.1088/1741-2560/10/5/056018.
[24] F. Shiman, E. López-Larraz, A. Sarasola-Sanz, N. Irastorza-Landa, M. Spüler, N. Birbaumer, and A. Ramos-Murguialday, "Classification of different reaching movements from the same limb using EEG," *J. Neural Eng.*, vol. 14, no. 4, Aug. 2017, Art. no. 046018, doi: 10.1088/1741-2552/aa70d2.
[25] E. Lew, R. Chavarriaga, S. Silvoni, and J. D. R. Millán, "Detection of self-paced reaching movement intention from EEG signals," *Frontiers Neuroeng.*, vol. 5, p. 13, Jul. 2012, doi: 10.3389/fneng.2012.00013.
[26] E. Y. L. Lew, R. Chavarriaga, S. Silvoni, and J. D. R. Millán, "Single trial prediction of self-paced reaching directions from EEG signals," *Frontiers Neurosci.*, vol. 8, p. 222, Aug. 2014, doi: 10.3389/fnins.2014.00222.
[27] H. Kim, N. Yoshimura, and Y. Koike, "Classification of movement intention using independent components of premovement EEG," *Frontiers Hum. Neurosci.*, vol. 13, p. 63, Feb. 2019, doi: 10.3389/fnhum.2019.00063.
[28] V. Aggarwal, M. Mollazadeh, A. G. Davidson, M. H. Schieber, and N. V. Thakor, "State-based decoding of hand and finger kinematics using neuronal ensemble and LFP activity during dexterous reach-to-grasp movements," *J. Neurophysiol.*, vol. 109, no. 12, pp. 3067–3081, Jun. 2013, doi: 10.1152/jn.01038.2011.
[29] D. T. Bundy, M. Pahwa, N. Szrama, and E. C. Leuthardt, "Decoding three-dimensional reaching movements using electrocorticographic signals in humans," *J. Neural Eng.*, vol. 13, no. 2, Apr. 2016, Art. no. 026021.
[30] F. Faul, E. Erdfelder, A. G. Lang, and A. Buchner, "G* Power 3: A flexible statistical power analysis program for the social, behavioral, and biomedical sciences," *Behav. Res. Methods*, vol. 39, no. 2, pp. 175–191, 2007.
[31] T. Chouhan, N. Robinson, A. P. Vinod, K. K. Ang, and C. Guan, "Wavlet phase-locking based binary classification of hand movement directions from EEG," *J. Neural Eng.*, vol. 15, no. 6, Dec. 2018, Art. no. 066008, doi: 10.1088/1741-2552/aadeed.
[32] M. A. Klados, C. Papadelis, C. Braun, and P. D. Bamidis, "REG-ICA: A hybrid methodology combining blind source separation and regression techniques for the rejection of ocular artifacts," *Biomed. Signal Process. Control*, vol. 6, no. 3, pp. 291–300, Jul. 2011, doi: 10.1016/j.bspc.2011.02.001.
[33] A. Delorme and S. Makeig, "EEGLAB: An open source toolbox for analysis of single-trial EEG dynamics including independent component analysis," *J. Neurosci. Methods*, vol. 134, no. 1, pp. 9–21, Mar. 2004, doi: 10.1016/j.jneumeth.2003.10.009.
[34] C. Carvalhaes and J. A. de Barros, "The surface Laplacian technique in EEG: Theory and methods," *Int. J. Psychophysiol.*, vol. 97, no. 3, pp. 174–188, Sep. 2015, doi: 10.1016/j.ijpsycho.2015.04.023.
[35] H. Ramoser, J. Müller-Gerking, and G. Pfurtscheller, "Optimal spatial filtering of single trial EEG during imagined hand movement," *IEEE Trans. Neural Syst. Rehabil. Eng.*, vol. 8, no. 4, pp. 441–446, Dec. 2000.
[36] F. Lotte and C. Guan, "Regularizing common spatial patterns to improve BCI designs: Unified theory and new algorithms," *IEEE Trans. Biomed. Eng.*, vol. 58, no. 2, pp. 355–362, Feb. 2011, doi: 10.1109/TBME.2010.2082539.
[37] C. E. Rasmussen, "Gaussian processes in machine learning," in *Proc. Summer School Mach. Learn.*, Lecture Notes in Computer Science: Including Subseries Lecture Notes in Artificial Intelligence and Lecture Notes in Bioinformatics, vol. 3176, 2004, pp. 63–71, doi: 10.1007/978-3-540-28650-9_4.
[38] C. E. Rasmussen and C. K. I. Williams, *Gaussian Processes for Machine Learning*. Cambridge, MA, USA: MIT Press, 2006.
[39] A. Kraskov, H. Stögbauer, and P. Grassberger, "Estimating mutual information," *Phys. Rev. E, Stat. Phys. Plasmas Fluids Relat. Interdiscip. Top.*, vol. 69, no. 6, p. 16, Jun. 2004, doi: 10.1103/PhysRevE.69.066138.
[40] J. M. Antelis, L. Montesano, A. Ramos-Murguialday, N. Birbaumer, and J. Minguez, "On the usage of linear regression models to reconstruct limb kinematics from low frequency EEG signals," *PLoS ONE*, vol. 8, no. 4, Apr. 2013, Art. no. e61976, doi: 10.1371/journal.pone.0061976.
[41] T. Hastie, R. Tibshirani, and J. Friedman, *The Elements of Statistical Learning: Data Mining, Inference, and Prediction*. New York, NY, USA: Springer, 2009.
[42] D. Simon, *Optimal State Estimation: Kalman, H∞, and Nonlinear Approaches*. Hoboken, NJ, USA: Hoboken, NJ, USA: Wiley, 2006.
[43] H. Drucker, C. J. C. Burges, L. Kaufman, A. Smola, and V. Vapnik, "Support vector regression machines," in *Proc. Adv. Neural Inf. Process. Syst.*, vol. 9, 1996, pp. 1–7.

[44] A. Khorasani, N. H. Beni, V. Shalchyan, and M. R. Daliri, "Continuous force decoding from local field potentials of the primary motor cortex in freely moving rats," *Sci. Rep.*, vol. 6, no. 1, pp. 1–10, Oct. 2016, doi: 10.1038/srep35238.
[45] A. Ahmadi, A. Khorasani, V. Shalchyan, and M. R. Daliri, "State-based decoding of force signals from multi-channel local field potentials," *IEEE Access*, vol. 8, pp. 159089–159099, 2020, doi: 10.1109/ACCESS.2020.3019267.
[46] N. Terry and Y. Choe, "Splitting Gaussian processes for computationally-efficient regression," *PLoS ONE*, vol. 16, no. 8, Aug. 2021, Art. no. e0256470, doi: 10.1371/journal.pone.0256470.
[47] J. L. Contreras-Vidal and S. E. Kerick, "Independent component analysis of dynamic brain responses during visuomotor adaptation," *NeuroImage*, vol. 21, no. 3, pp. 936–945, Mar. 2004, doi: 10.1016/j.neuroimage.2003.10.037.
[48] Y. Wang and S. Makeig, "Predicting intended movement direction using EEG from human posterior parietal cortex," in *Proc. Int. Conf. Found. Augmented Cogn.*, 2009, pp. 437–446, doi: 10.1007/978-3-642-02812-0_52.
[49] R. D. Flint, M. C. Tate, K. Li, J. W. Templer, J. M. Rosenow, C. Pandarinath, and M. W. Slutzky, "The representation of finger movement and force in human motor and premotor cortices," *Eneuro*, vol. 7, no. 4, Jul. 2020.
[50] W. Wu, Y. Gao, E. Bienenstock, J. P. Donoghue, and M. J. Black, "Bayesian population decoding of motor cortical activity using a Kalman filter," *Neural Comput.*, vol. 18, no. 1, pp. 80–118, 2006, doi: 10.1162/089976606774841585.
[51] J.-H. Kim, F. Biessmann, and S.-W. Lee, "Decoding three-dimensional trajectory of executed and imagined arm movements from electroencephalogram signals," *IEEE Trans. Neural Syst. Rehabil. Eng.*, vol. 23, no. 5, pp. 867–876, Sep. 2015, doi: 10.1109/TNSRE.2014.2375879.
[52] R. J. Kobler, A. I. Sburlea, V. Mondini, M. Hirata, and G. R. Müller-Putz, "Distance- and speed-informed kinematics decoding improves M/EEG based upper-limb movement decoder accuracy," *J. Neural Eng.*, vol. 17, no. 5, Nov. 2020, Art. no. 056027, doi: 10.1088/1741-2552/abb3b3.
[53] J.-H. Jeong, K.-H. Shim, D.-J. Kim, and S.-W. Lee, "Brain-controlled robotic arm system based on multi-directional CNN-BiLSTM network using EEG signals," *IEEE Trans. Neural Syst. Rehabil. Eng.*, vol. 28, no. 5, pp. 1226–1238, May 2020, doi: 10.1109/TNSRE.2020.2981659.
[54] Y. Benjamini, A. M. Krieger, and D. Yekutieli, "Adaptive linear step-up procedures that control the false discovery rate," *Biometrika*, vol. 93, no. 3, pp. 491–507, Sep. 2006, doi: 10.1093/biomet/93.3.491.

SEYYED MOOSA HOSSEINI received the B.S. degree in electrical engineering from the Amirkabir University of Technology (AUT), Tehran, Iran, in 2012, and the M.S. degree in communication engineering from the K. N. Toosi University of Technology (KNTU), Tehran, in 2014. He is currently pursuing the Ph.D. degree in electrical engineering with the Iran University of Science & Technology (IUST). His research interests include brain–computer interfaces (BCI), neural signal processing, and biomedical engineering.

VAHID SHALCHYAN received the M.Sc. degree in biomedical engineering from the Amirkabir University of Technology, Tehran, Iran, in 2002, and the Ph.D. degree in biomedical science and engineering from Aalborg University, Aalborg, Denmark, in 2013. From 2011 to 2013, he was a Visiting Researcher with the University Medical Center Göttingen, Georg-August University, Göttingen, Germany. He has been an Associate Professor with the Department of Biomedical Engineering, School of Electrical Engineering, Iran University of Science & Technology (IUST), Tehran. His research interests include biomedical signal processing and pattern recognition, with an emphasis on their application to neural signals, for neuroscience, neurotechnology, and brain–computer interface researches.